

Feasibility Analysis of a Spiral Groove Ring Seal for Counter-Rotating Shafts

Eliseo DiRusso*

NASA Lewis Research Center, Cleveland, Ohio

A feasibility analysis was performed on the use of spiral-groove gas bearings in a ring seal between counter rotating shafts in advanced turbofan engines. The analysis focused on the lift force characteristics of the spiral grooves for steady state conditions. A computer program for predicting the performance of gas lubricated face seals was used to optimize the spiral groove geometry to produce maximum lift force. Load capacity curves (lift force as a function of film thickness) were generated for four advanced turbofan engine operating conditions at relative seal speeds ranging from 17,850 to 29,800 rpm, sealed air pressures from 6 to 42 N/cm² (9 to 60 psi) absolute, and temperatures from 95 to 327 °C (203 to 620 °F). The relative seal sliding speed range was 152 to 255 m/s (500 to 836 ft/s). The analysis showed that the spiral grooves are capable of producing sufficient lift force under steady state conditions such that the ring seal will operate in a noncontacting mode over the operating range of typical advanced turbofan engines.

Introduction

THE spiral groove intershaft ring seal shown in Fig. 1 is a new seal concept which has potential application in sealing fan bleed air between two counter rotating shafts in advanced turbofan aircraft engines. This is a difficult sealing application for any contacting type seal because the counter rotating shafts set up very high sliding speeds for the seal which are on the order of 259 m/s (850 ft/s). In addition to the high sliding speed, the seal must accommodate approximately 0.64 cm (0.25 in.) of axial translation due to relative axial motion between the two shafts.

The intershaft ring seal application is an excellent example of the need for applying self acting gas lubricated bearing technology to contacting-type seals. Application of a gas bearing in the form of spiral grooves to the faces of the ring seal housing (Fig. 1) will maintain a thin air film of relatively high stiffness between the seal ring and the housing, thereby enabling the seal to operate in a noncontacting mode over the entire engine operating range. The seal could then potentially operate at 259 m/s (850 ft/s) sliding speed, accommodate axial translations of 0.64 cm (0.25 in.), and have leakage rates consistent with contacting type seals.

When spiral grooves are employed in a seal as a film generating mechanism, the following are generally required in order to calculate the axial force equilibrium: 1) film load capacity curve (lift force as function of film thickness), 2) minimum film thickness over the operating range, and 3) optimization of the spiral groove geometry to maximize the lift force for a given seal envelope size and operating condition.

The objective of this analysis is to determine the feasibility of using spiral grooves in the intershaft seal and to calculate the load capacity curves, calculate minimum film thickness (for steady state) over a typical turbofan engine operating range, and to optimize the spiral groove geometry to produce maximum lift force for a given seal envelope size. A computer program¹ was employed to achieve these objectives analytically.

Discussion and Analysis

Seal Operating Features

Figure 1 shows the intershaft seal concept chosen for this study. The housing which contains the carbon ring rotates with the inner shaft. The carbon ring is bounded on its outside diameter by the outer shaft which counter rotates with respect to the inner shaft. As the shafts rotate, the carbon ring expands into the outer shaft and assumes the speed of the outer shaft. The relative sliding speed between the carbon ring and the inner shaft can approach 259 m/s (850 ft/s). It should be noted that the carbon ring may require a radial split line to limit hoop stresses due to rotation and to assure that the carbon ring will rotate with the outer shaft. The effect of the split in the ring on the spiral groove performance in the region of the gap is not known and is an area for future investigation. Also close attention must be given to the mechanical design of the split line to assure smooth mechanical operation with minimum compromise of spiral groove performance.

Relative axial translations between the inner and outer shafts of up to 0.64 cm (0.25 in.) due to thermal expansion are possible over the design operating range. This translation causes the carbon ring to approach one of the two housing faces. The spiral grooves on the housing faces generate a very high lift force as the carbon ring approaches either face, thereby maintaining a fluid film between the carbon ring and the housing face.

Figure 2 is a schematic drawing of the seal showing it in a neutral position (equal clearance on either side of the carbon). The total axial clearance between the carbon ring and the housing face is 0.0203 mm (0.0008 in.) or 0.0102 mm (0.0004 in.) per side when the seal is centered in the housing. The air flow through the seal is shown in Fig. 2. P_1 is the high pressure and the pressure drop from P_1 to P_2 occurs across the seal dam. The porting shown in Fig. 2 is designed such that the spiral grooves are bounded by the sealed pressure (P_1) at both the outside and inside diameters, hence, there is no pressure difference across the spiral grooves. This is known as a pressure balanced spiral groove concept. The pressure balanced concept isolates the spiral groove flow from the seal leakage flow so that the spiral groove performance is not subject to any ill effects due to seal leakage flow.

Transients such as pressure and thermal expansion which occur over the engine operating range will change the axial

Received March 8, 1983; revision received March 20, 1984. This paper is declared a work of the U.S. Government and therefore is in the public domain.

*Mechanical Engineer

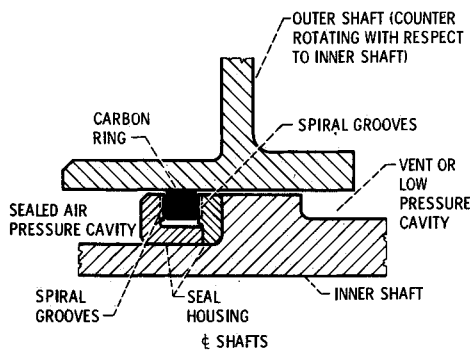


Fig 1 Spiral groove intershaft seal

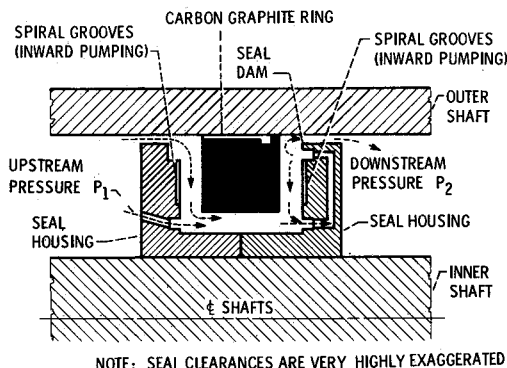


Fig 2 Schematic of intershaft ring seal

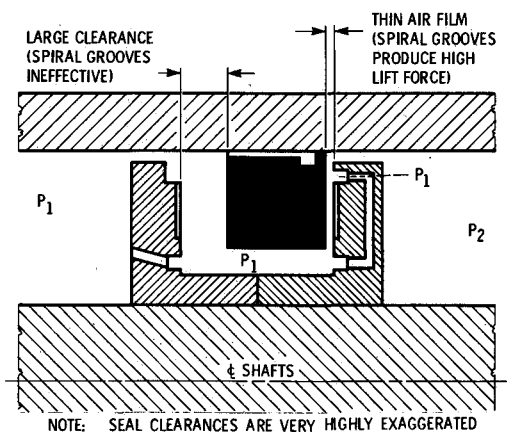


Fig 3 Schematic showing seal ring displaced toward housing face

force equilibrium of the seal, thus causing the carbon seal ring to approach one of the housing faces as shown in Fig 3. As the clearance between the carbon seal ring and one of the housing faces approaches zero clearance, the spiral grooves generate a very high lift force. The lift force increases exponentially with reduction in clearance until a clearance is achieved at which axial force equilibrium is restored. The forces which enter into the axial force equilibrium are pressure area forces on the carbon ring, friction force between the carbon ring and the outer shaft (produced by relative axial translations of the shafts), and the lift force generated by the spiral grooves.

Spiral Groove Analysis

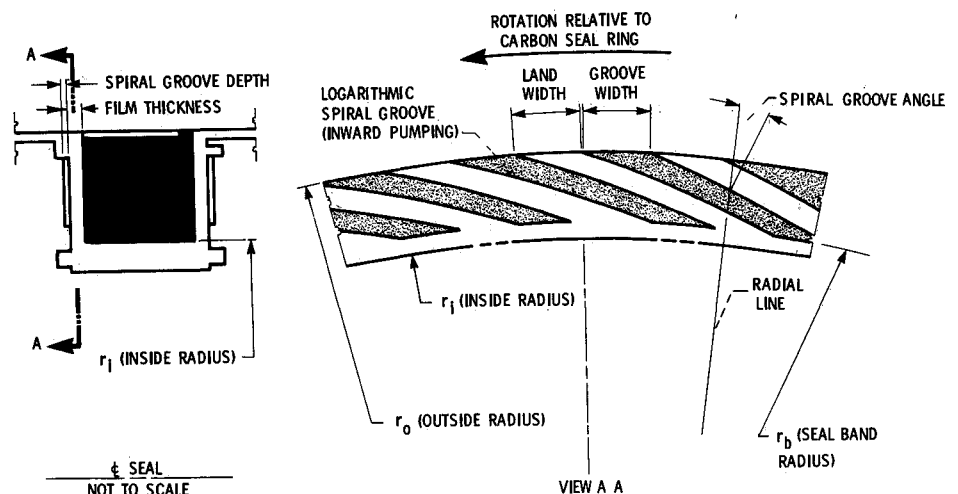
As stated previously, the analysis was directed to predicting the spiral groove load capacity curves and to optimize the spiral groove geometry for steady state conditions. A computer program¹ was used in the analysis. The program predicts the performance of spiral groove gas lubricated (compressible fluid) face seals for either inward or outward pumping spiral groove configurations, the form of which is logarithmic spirals. An inward pumping spiral groove configuration pumps the fluid radially from the outer region of the seal toward the center; conversely, an outward pumping configuration pumps the fluid radially from the inner region of the seal toward the outside. Inputs to the program are spiral groove geometric data, misalignment angles, speed, fluid viscosity, temperatures and pressures. Outputs which were used were fluid film lift force, film thickness, and pressure distribution.

The film pressure profile is calculated by solving the governing fluid equation (Reynolds equation) using a converging finite difference approximation. The analytical treatment is based on the narrow groove theory² modified for logarithmic spiral groove geometry.

The seal ring and spiral groove geometry are shown in Fig. 4. The inside and outside diameters of the seal ring were set by the available space in a typical advanced turbfan engine. The spiral-groove outside radius r_o and the seal band radius r_b were selected to maximize the radial length of the spiral grooves ($r_o - r_b$) within the available radial space. The bearing dam width ($r_b - r_i$) of 0.10 cm (0.04 in.) was selected as a practical minimum. Optimizing studies on this parameter have not been done since it was found that maximizing ($r_o - r_b$) produced the highest lift. Having specified the above parameters, the spiral groove depth, spiral groove angle and groove to land width ratio are left as the lift force optimizing parameters. The spiral groove optimization was carried out for engine operating condition 1 (see Table 1).

Figure 5 is a plot of spiral groove depth for maximum lift force as a function of film thickness. Data for this plot were

Fig 4 Spiral groove ring seal geometry and nomenclature



obtained by generating a family of curves of lift force as a function of groove depth. The groove depth associated with the maximum lift force for each film thickness then was taken from this family of curves and plotted against their respective film thicknesses. The plot shows that the maximum lift force occurs at a film thickness to groove depth ratio of approximately 0.29 for film thicknesses above approximately 0.0025 mm (0.0001 in.). Although this curve was plotted using the optimized conditions of this analysis, it applies generally for spiral-groove seals.

The desired operating film thickness was set at 0.0051 mm (0.0002 in.), hence the groove depth according to Fig. 5 should be 0.0178 mm (0.0007 in.) for maximum lift force to occur at 0.0051 mm (0.0002 in.) film thickness. Computer runs then were made for a groove depth of 0.0178 mm (0.0007 in.) to determine the combination of spiral groove angle and groove to land width ratio at which the maximum lift force occurs. Figure 6 is a plot of lift force as a function of spiral

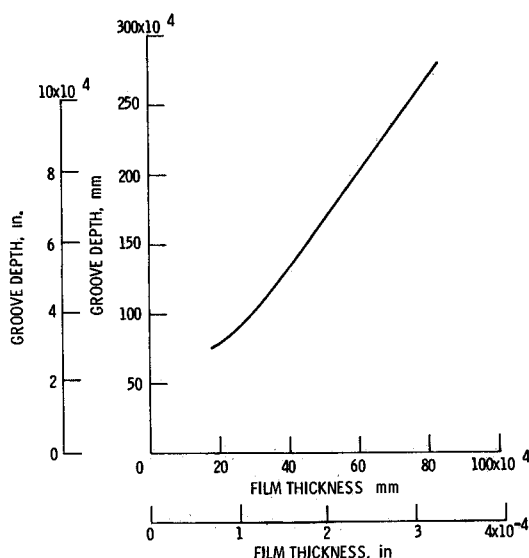


Fig. 5 Groove depth for maximum lift force as function of film thickness

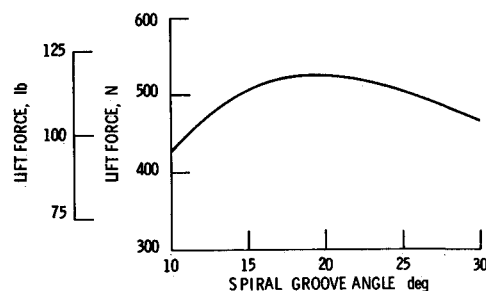


Fig. 6 Lift force as function of spiral groove angle

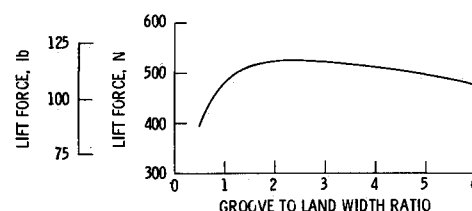


Fig. 7 Lift force as function of groove to land width ratio

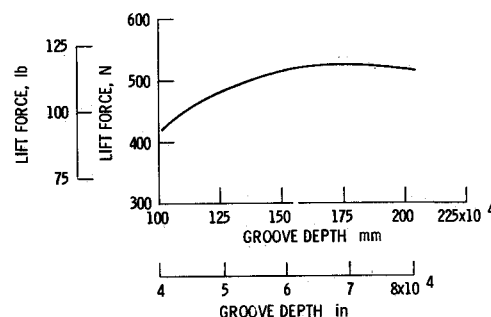


Fig. 8 Lift force as function of groove depth

Table 1 Typical seal environmental conditions for various engine operating conditions

Engine operating condition	Sealed air pressure P_1 , absolute, N/cm ² (psi)	Sealed air temperature T_1 , C (F)	Downstream air pressure P_2 , absolute, N/cm ² (psi)	Downstream air temperature, T_2 , C (F)	Sealed air viscosity N s/cm ² (lbf s/in. ²) $\times 10^{-8}$	Relative seal speed, ^a rpm
1	41.4 (60.0)	327 (620)	11.0 (16.0)	149 (300)	0.302 (0.438)	29,800
2	11.6 (16.8)	95 (203)	10.3 (15.0)	110 (230)	0.215 (0.312)	17,850
3	6.2 (9.0)	115 (239)	2.7 (3.9)	116 (240)	0.224 (0.325)	23,400
4	17.2 (25.0)	298 (569)	1.2 (1.7)	132 (270)	0.292 (0.424)	28,050

^aThe relative seal speed is the sum of the absolute speeds of the inner and outer shafts

Table 2 Operating film thickness ranges

Engine operating condition	Anticipated range of axial force which must be counteracted by spiral groove lift force, N (lb)	Operating film thickness range (from Fig. 11), mm (in.)
1	445-890 (100-200)	0.0037-0.0056 (0.00015-0.00022)
2	178-311 (40-70)	0.0042-0.0057 (0.00017-0.00022)
3	222-445 (50-100)	0.0038-0.0056 (0.00015-0.00022)
4	400-756 (90-170)	0.0038-0.0054 (0.00015-0.00021)

groove angle (all other parameters were held constant) The plot shows the lift force peaking out at approximately 20 deg Figure 7 is a plot of lift force as a function of groove to land width ratio (all other parameters were held constant) This plot shows the lift force peaking out at a groove to land width ratio of approximately 2.50 Figure 8 is a plot of lift force as a function of groove depth (all other parameters were held constant) This plot shows the lift force peaking out at a groove depth of approximately 0.0178 mm (0.0007 in.) as expected since this is the optimum groove depth for the 0.0051 mm (0.0002 in.) film thickness as discussed previously Note that for values of groove to land width ratio between 1.5 and 3, the lift force is rather insensitive to the groove to land width ratio Therefore for applications in which wear rate is critical, a groove to land width ratio of 1.5 can be selected instead of the optimum value of 2.5 with little reduction in lift force The lower groove to land width ratio increases the wear area which reduces the wear rate

The computer program used in the analysis assumed an infinite number of spiral grooves This assumption is justified when the number of grooves is 50 or more,³ hence, the previously calculated optimum parameters will be valid for any number of grooves over 50 The number of grooves must also comply with the assumptions of the narrow-groove theory² to be modeled accurately. The use of this theory is justified for groove aspect ratios (groove length to width ratio) greater than 5 Figure 9 shows the spiral grooves to scale for an 80 groove configuration The groove aspect ratio for the 80 groove configuration is approximately 8 and in agreement with the narrow groove assumption.

Figure 10 shows plots of lift force as a function of film thickness for operating condition 1 The dashed curve is for a constant film thickness to groove depth ratio of 0.29 and, therefore, shows the true optimum lift force for any given film thickness The solid curve gives the actual performance (compromised optimum lift force) for the constant groove depth of 0.0178 mm (0.0007 in.) This groove depth produces optimum lift force only at the desired operating film thickness of 0.0051 mm (0.0002 in.); hence, it is labeled as compromised optimum in Fig. 10 The curves illustrate the difference between the true optimum and the compromised optimum which results from the necessity of having to choose a unique groove depth for a specific design

Figure 11 shows lift force as a function of film thickness for the four operating conditions shown in Table 1 The lift force optimization was performed for engine operating condition 1; hence the lift force curve for this condition is optimum The

curves for engine operating conditions 2, 4 were calculated for the spiral groove angle, groove to land width ratio, and groove depth which were optimized for engine condition 1 Therefore, the curves for engine operating conditions 2, 4 are off design and are not necessarily optimum

The operating steady state film thickness range for each of the four operating conditions can be determined by consulting the appropriate curve in Fig. 11 The anticipated range of axial forces which must be counteracted by the spiral groove lift force is given in Table 2 These forces were estimated from conditions found in typical turbofan engines and the assumed coefficient of friction was 0.05 to 0.1 for carbon graphite on steel Entering the curves of Fig. 11 with these respective values of lift force yields the operating film thickness ranges shown in Table 2. The table shows that the minimum steady state film thickness found over the entire engine operating range was 0.0037 mm (0.00015 in.) and the average film thickness was 0.0047 mm (0.00019 in.)

This analysis addresses only the steady-state aspects of this type of seal In practice, however the seal will experience vibrations and misalignments which will modulate the steady state film thickness The dynamic response of this type of seal is obviously quite complex and is an area of future investigation

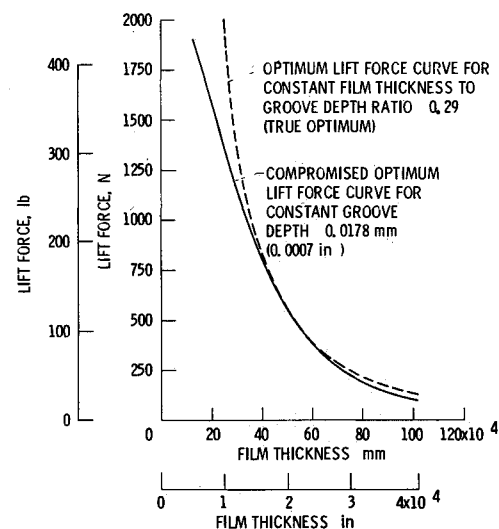


Fig. 10 Lift force as function of film thickness

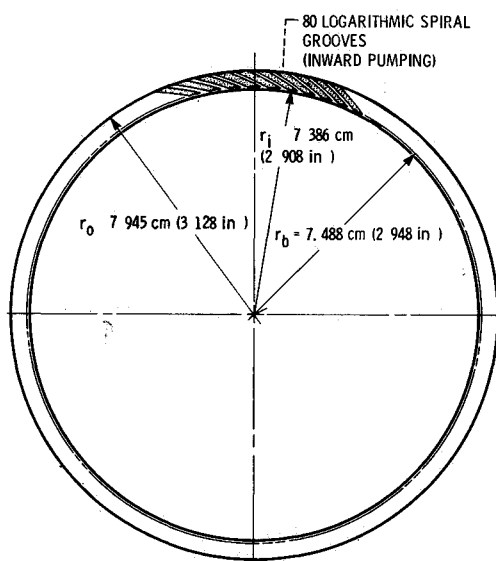


Fig. 9 Optimized logarithmic spiral grooves shown to scale

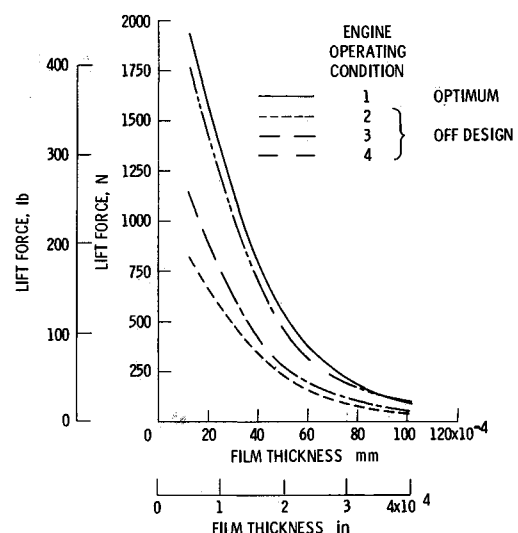


Fig. 11 Spiral groove load capacity curves.

Summary

An analysis was performed for a spiral-groove intershaft ring seal for turbofan engines to determine the lift characteristics of the spiral groove geometry for steady state conditions. The sealed fluid was air. A computer program¹ for predicting the performance of gas lubricated spiral-groove face seals was used to determine the optimum spiral groove geometry for maximum lift force and to generate load capacity curves (lift force as a function of film thickness).

The analysis produced the following results:

1) The spiral groove geometry can be optimized to produce sufficient lift force such that the ring seal will operate in a noncontacting mode for steady-state conditions even with the space limitation of typical advanced turbofan engine intershaft seal applications.

2) The minimum steady state film thickness over the entire anticipated advanced turbofan engine operating range was 0.0037 mm (0.00015 in.) and the average film thickness was approximately 0.0047 mm (0.00019 in.), which is satisfactory for this application.

3) The following optimum values of the spiral groove geometrical features were found to produce maximum lift force for engine operating condition 1 (see Table 1): groove

depth, 0.0178 mm (0.0007 in.) [this value of groove depth is optimum for a film thickness of 0.0051 mm (0.0002 in.)]; spiral groove angle, 20 deg; groove to land width ratio, 2.50.

To reduce leakage it is advantageous to use a low leakage contacting type seal instead of a labyrinth for the intershaft seal in advanced turbofan engines. The inherently high sliding speed [259 m/s (850 ft/s)] of intershaft seals produces very high friction and wear in contacting-type seals using conventional materials. The use of spiral grooves enables a contacting-type seal to operate in a noncontacting mode thereby eliminating the friction and wear problems and permitting the use of conventional seal materials at these speeds.

References

- ¹ 'Spiral Groove Face Seal Computer Program (SEALSG)', Mechanical Engineering Laboratory, Franklin Research Center, Philadelphia, Pa., Project 21464, March 1979.
- ² Elrod, H. G., 'A Generalized Narrow Groove Theory for the Gas Lubricated Herringbone Thrust Bearing', *Proceedings of the Fourth Gas Bearing Symposium*, Vol. 2, Univ. of Southampton, England, April 1969, pp. 18-1 to 18-21.
- ³ Muijderland, E. A., *Spiral Groove Bearings*, Springer Verlag, New York, 1966.

From the AIAA Progress in Astronautics and Aeronautics Series.

COMBUSTION EXPERIMENTS IN A ZERO-GRAVITY LABORATORY—v. 73

Edited by Thomas H. Cochran, NASA Lewis Research Center

Scientists throughout the world are eagerly awaiting the new opportunities for scientific research that will be available with the advent of the U.S. Space Shuttle. One of the many types of payloads envisioned for placement in earth orbit is a space laboratory which would be carried into space by the Orbiter and equipped for carrying out selected scientific experiments. Testing would be conducted by trained scientist astronauts on board in cooperation with research scientists on the ground who would have conceived and planned the experiments. The U.S. National Aeronautics and Space Administration (NASA) plans to invite the scientific community on a broad national and international scale to participate in utilizing Spacelab for scientific research. Described in this volume are some of the basic experiments in combustion which are being considered for eventual study in Spacelab. Similar initial planning is underway under NASA sponsorship in other fields—fluid mechanics, materials science, large structures, etc. It is the intention of AIAA in publishing this volume on combustion in zero gravity to stimulate by illustrative example new thought on kinds of basic experiments which might be usefully performed in the unique environment to be provided by Spacelab, i.e., long term zero gravity, unimpeded solar radiation, ultra high vacuum, fast pump out rates, intense far ultraviolet radiation, very clear optical conditions, unlimited outside dimensions, etc. It is our hope that the volume will be studied by potential investigators in many fields, not only combustion science, to see what new ideas may emerge in both fundamental and applied science, and to take advantage of the new laboratory possibilities.

280 pp. 6×9 illus., \$20.00 Mem. \$35.00 List

TO ORDER WRITE: Publications Order Dept., AIAA, 1633 Broadway, New York, N.Y. 10019